



Near-edge elastic photon scattering from dilute aqueous ions

D.A. Bradley^a, R.P. Hugtenburg^{b,*}, A.L. Yusoff^a

^a*School of Physics, University of Exeter, Exeter, EX4 6HU, UK*

^b*Queen Elizabeth Medical Centre, University Hospital Birmingham, B15 2TH, UK/ School of Physics and Astronomy, University of Birmingham, B15 2TT, UK*

Received 2 February 2005; accepted 28 December 2005

Abstract

For ions in aqueous solutions, measurements of elastic photon scattering cross-sections have been made in the vicinity of core atomic orbital energies. It is proposed that the aqueous system provides a suitable situation for testing predictions obtained through use of the independent particle approximation (IPA); using intermediate atomic number elements, and at ionic concentrations ranging from 0.01 to 0.1 M/l, resonance structures accord with predictions of elastic scattering cross-sections calculated within IPA. Conversely, at higher ionic concentrations (>0.1 M/l) the resonance structure is distorted. The amplitudes calculated using modified form-factors and anomalous scatter factors computed from a Slater exchange potential, were convolved with a Lorentzian of several eV. This results in cancellation of the increasingly rapid fluctuations, producing a smoothly continuous cross-section across the ionisation threshold. © 2006 Elsevier Ltd. All rights reserved.

Keywords: Rayleigh scattering; K-edge; Charge state

1. Introduction

In attempting to solve the structure of molecules, it is a matter of record that the isomorphous replacement technique in combination with use of anomalous Rayleigh scattering (dispersion in the vicinity of atomic orbital edges) allowed the absolute configuration of the naturally occurring chiral molecule tartaric acid to be obtained (Bijvoet, 1949; Bijvoet et al., 1951). The methodology has since been widely adopted by structural biologists in overcoming the so-called phase problem (Templeton, 1994). In support of the methodology a number of important tabulations of anomalous scatter-

ing factors exist (Cromer and Liberman, 1970; Cullen, 1989; Kissel, 2000).

Few direct measurements of the intensity of anomalous elastic photon-atom scattering within the edge exist, being due to difficulties in correcting for target size, attenuation and source profile. As such, indirect techniques have been employed, in particular interferometry (e.g., Creagh, 1984). Recently, in exploratory studies conducted by this group, direct measurement of anomalous scatter cross-sections have been attempted for a number of elements over a limited photon energy range, scanning the photon energy from just below the absorption-edge of interest (to-date this group have focused on anomalous photon-atom scattering in the region of the K-edge). Attenuation effects have been minimised by employing dilute salt solutions and also thin films of the associated neutral metals. Particular interest concerns sensitivity of the below edge structure to the ionic state of the elements Cu and

*Corresponding author. Tel. +44 121 414 4664; fax: +44 121 627 2386.

E-mail address: r.p.hugtenbung@bung.ac.uk (R.P. Hugtenburg).

Zn, as well as several other elements which are known to have important biomedical roles, also including applications in dosimetry. The sensitivity is clearly due to changes in the occupancy of outer orbitals.

For experiments, use has been made of synchrotron radiation (Hugtenburg et al., 2002; Hugtenburg and Bradley, 2004; Hugtenburg et al., 2004), benefitting from the tunability, inherently high optical stability and brightness of such beams. From such studies, confirmation of predictions from the independent atom approximation have been obtained, in particular of the oscillatory nature of below-edge structure due to bound-bound resonant intermediates. We have further sought to examine the influence of atomic and oxidation number on the size and structure of bound-bound resonant peaks. General trends, predicted within the independent particle approximation (Zhou et al., 1990; 1992; Carney et al., 2000) have been confirmed including increase in the size of bound-bound resonances with decreasing Z and with increased ionisation state.

Fig. 1, plots oscillator strengths for several atoms and ions utilised in our studies and calculated for a Dirac–Slater exchange potential with a Latter tail using RTAB. The trend as a function of atomic number and charge demonstrates the particular relevance of the process to low- Z electrolytes, as in for instance those of biological systems, dopants in glass, and indicates further importance for a range of catalysts. The strong dependence of oscillator strength upon charge state promises interesting possibilities for application of anomalous scattering to low- Z molecular components, normally rendered infeasible due to the rapid attenuation of X-rays at the K-edge of such elements.

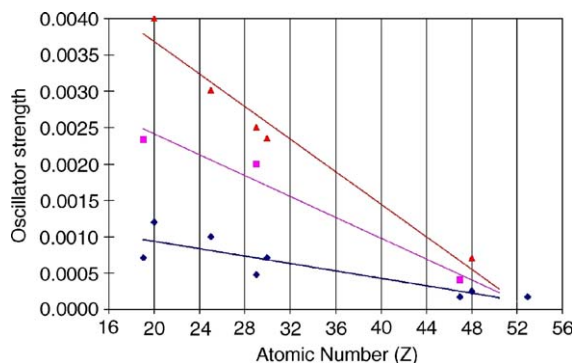


Fig. 1. General trend in oscillator strength as a function of Z and charge (diamonds are neutral, squares are +1, triangles are +2, the lines indicate the trend. Cross-sections at the bound-bound resonance peaks accord with the square of the oscillator strength which is a function of complex orbital structure.

2. Theoretical considerations

While previous synchrotron studies utilising fine structure in anomalous diffraction have been greatly successful, the fine structure of interest is above edge and corresponds to interatomic effects. The current work focuses on fine structure entirely generated by an atomic effect and predicted within the confines of the independent atomic model, with electronic configurations defined by the Dirac–Slater exchange potential (Lieberman et al., 1971). Bound-bound resonance occurs with the summing of intermediates associated with the Rayleigh scatter amplitude, being physical when a bound electron has access to an unoccupied orbital. In the case of neutral and chemically ionised systems this involves transition to a higher energy state, resonances occurring for bound electrons at energies several eV's or more in excess of associated below-edge emissions such as resonant X-ray Raman scattering are of interest in near-edge X-ray absorption and fluorescence analysis (e.g., XANES) and treated in detail elsewhere (Stohr, 1998; Hamalainen et al., 1989).

Rayleigh scattering, the elastic scattering of photons by atomic orbital electrons, can be accurately modelled within the independent particle approximation (IPA) over a wide range of scattering angles and energies using second order S-matrix methods (Kissel et al., 1995). This method is computationally intensive requiring the evaluation of slowly converging integrals of all possible allowed and forbidden transitions. It is therefore pertinent that form-factor methods with anomalous scattering factor corrections have been shown to be an adequate substitute for a restricted set of scattering conditions, in particular, for forward angle scattering (Kissel et al., 1995; Bradley et al., 1999). Additionally, use of form factors has been justified in obtaining outer electron contributions to scattering amplitudes, combining these with S-matrix computations for inner electrons in obtaining the elastic scattering cross-section. While high-resolution evaluations of the form-factor approximation exist, including anomalous scattering factor (ASF) corrections (see below for a brief discussion of this), no systematic evaluations of S-matrix computed cross-sections have been attempted that would enable close scrutiny of near-edge structure. ASF provides a qualitative guide to this energy dependent structure in the vicinity of the atomic orbital binding energies. The construction, based on the Kramer–Kronig relations, is a composite of two resonant absorption effects, that of photoionisation and photo-excitation. With the generation of life-time (Lorentzian) broadened cross-sections, photo-ionisation leads to the familiar broad minima in the Rayleigh scattering cross-section centred on the ionisation threshold; photo-excitation or bound-bound resonance introduces a significant constant contribution to the cross-section as well as rapid fluctuations at each

oscillator energy, forming a Rydberg series of maxima and minima that become smoothly varying in approach to the ionisation threshold.

In the studies reported herein we focus on measurement and evaluation of the near-edge structure for atoms and ions in the aqueous system, dominated below edge by bound-bound resonance.

3. Methodology

Through knowledge of the electronic structures associated with the aqueous system we are able to assess the validity of using IPA. The experimental work has been divided into two parts; in the first, photon scattering from thin vapour-deposited metals on suitable substrates has been explored, while in the second, photon scattering dilute aqueous systems have been examined. Both systems resolve issues with regard to the difficulty in defining target dimensions. Pilot studies were performed at one or other of two stations at the synchrotron radiation source (SRS), Daresbury Laboratories, this being a second generation machine; Station 16.3 provides fine collimation of the scattering angle, also allowing the change in Rayleigh scatter cross-section to be measured at constant momentum transfer for on-sample photon energies that are made to vary. This makes it ideal for crystalline or metallic systems. Station 16.5 has a wide acceptance angle, being appropriate for amorphous systems; change in cross-section with incident photon energy can be obtained at a constant angle. In both cases the incident X-rays were selected with a dual Si monochromator in the [220] orientation giving a relative bandwidth of $\Delta E/E = 7.44 \times 10^{-5}$.

The approach has already been successfully used by others, in particular using dual gas cells (Young et al., 2001), suggesting that in the vicinity of atomic edges scattering from a reference atomic system can be used to calibrate relative cross-sections. Extension to the aqueous environment now has the medium acting as the reference system, offering challenges, in particular photons scattered by the medium being absorbed by the ion. This ultimately limits the thickness of the attenuating medium and motivates the use of bright synchrotron photon sources. For more recent measurements, tuneable X-rays have been obtained at satisfactory brightness and eV resolution using a [111] Si monochromator, at bending magnet station BM28 at the ESRF, a third generation machine. From Cu and Zn ions in aqueous solutions, the X-rays were scattered through high angles, the medium being contained in a thin perspex cell containing 8 μm kaplan windows. An HPGe detector was used to collect the scattered signal, providing an energy resolution of about 500 eV, being adequate to separate the elastic scattering signal from

K_{α} radiation but not from Compton or K_{β} contributions. The slowly varying Compton (A^2) contribution from the medium was removed by assuming validity of the relativistic impulse approximation. The contribution due to K_{β} fluorescence was handled by assuming the branching ratio for K_{α} and K_{β} contributions to be constant and to be described accurately by fluorescent yields measured above edge. The assumption that the K_{β} contribution has a functionally similar dependency with incident energy to the well-resolved K_{α} contribution above edge, as well as variations in resonant Raman scattering components below edge, has not yet been verified near-edge but has precedent in the utilisation of photoeffect fluorescent yield in XANES analysis, as shown for instance by Suorrti (1979). Measurements were conducted over a limited energy range in order to satisfy constraints imposed by the stability of the measurement system.

The metals films, deposited on glass, have a nominal thickness of approximately 100 nm. An optimum orientation can be determined via scans over a wide angular range, selecting from this predominant reflections, respectively at [1 1 1] and [2 2 2], from which to measure scatter intensities at a constant momentum transfer.

For the ionic solutions, investigations were made for a range of dilutions, from several tens of parts per million (ppm) through to several hundred ppm. Detection was obtained through use of a cryogenically cooled hyper-pure germanium (HPGe), for a large ($> 10^\circ$) acceptance angle appropriate for the low relative count rate of the target element within the aqueous medium.

The measured intensities have been compared to cross-sections determined using the low energy form of the Kramer–Kronig dispersion integrals. High precision in the determination of cross-sections from experiment have been achieved by evaluation relative to cross-sections obtained typically 50 eV either side of the edge which in general have been experimentally confirmed. This assumption may lead to small inaccuracies above edge due to the presence of environmentally related oscillations.

Total photoeffect cross-sections, modified form-factors and bound-bound oscillator strengths have been determined within a relativistic Dirac–Slater potential with a Latter tail. Code based on HEX (Liebermann et al., 1971) has been used to compute a self-consistent potential for neutral and positively ionised atoms. The photoeffect evaluation adapted from code written by Scofield (1973) considers only the photoionisation channel which is satisfactory except below edge where resonant Raman scatter and bound-bound excitations occur at comparable amplitudes. The latter have been computed following formalism due also to Scofield (1969).

4. Results and discussion

Our results concur with the most common method of measurements of anomalous scattering, determined for thin crystalline samples or vapour-deposited metallic material. As previously referred to, solutions give access to ionic states, several examples of simple molecular systems possessing effectively a neutral coordination in an amorphous arrangement. Example results for such a situation, for scattering for a 3.7 mg/ml solution of molecular iodine, are shown in Fig. 2 (Hugtenburg et al., 2002) comparing measured data with IPA theory updating the data presented in the original publication with the inclusion of 5 eV Lorentzian lifetime broadening.

The measurements agree qualitatively with the predicted cross-sections. The energy of the minimum at 10 ± 5 eV below the K-edge (33.164 keV) is in reasonable agreement with the ASF prediction (10.2 eV) which incorporates a small influence of the below-edge bound-bound resonance structure. The Rayleigh scatter differential cross-section for iodine in the vicinity of the K-edge, determined from measurements of this dilute solution, have been compared to that using relativistic form factors with ASF corrections from an existing

database (solid line). The error bars give the statistical error (2σ) due predominantly to Rayleigh scattering in the medium and background sources. Clearly improved statistics are required; as previously mentioned, while these pilot study data were obtained at the Second generation Daresbury SRS, further research has made use of the Third generation ESRF synchrotron source, located in Grenoble; in particular at ESRF beamline BM28, the potential exists for an intensity improvement of ~ 70 times over that obtained at Daresbury beamline 16.3, with which it otherwise shares similar beam characteristics.

Other recently published work concerns measurements of near-edge Rayleigh scatter for dilute transition metal ion solutions (Hugtenburg et al., 2004) demonstrating the increased influence of both charge state and Z value on the size of the bound-bound oscillations (supporting the predicted trend shown in Fig. 1). The results suggest a role for the bound-bound contributions, known to be important for atoms and ions, with valence configurations that allow transitions from a bound s orbital to an unoccupied 4p-orbital or below. In these circumstance bound-bound oscillations generate minima several 10's of eV below the real position of the

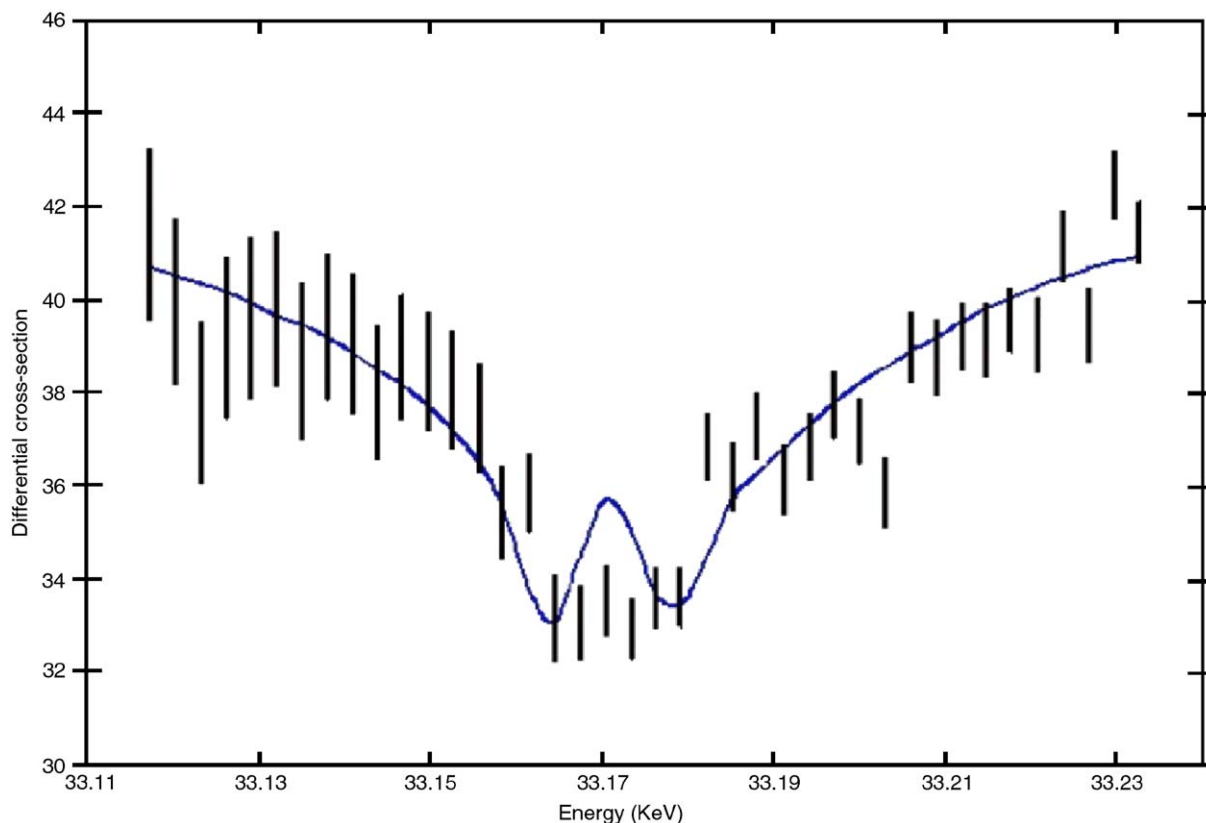


Fig. 2. Results of pilot investigation for molecular iodine, showing structure near the K-absorption edge at (33.164 keV).

edge. In direct analogy to photo excitation we anticipate that the bound–bound resonance structure offers a probe of the unoccupied state. We note that the resonance occurs at high resolutions (within several eV of the edge), being demonstrable with monochromatic beams provided by SRS. The predicted rapid variation in the below-edge scattering structure should be distinguishable from various background interference including edge-related inelastic scatter effects such as resonant Raman scatter which occur at lower energies, corresponding to transitions between occupied orbitals, and environmental effects (as seen through use of the synchrotron-based techniques XANES and EXAFS) which occur above edge.

Discrepancies with predictions, in particular broadening, are to be anticipated in the dilute aqueous system, being suggestive of complex effects; our results for Cu

show the strongest resonance from 1s to 4p and 5p transitions to be broadened (by around 5 eV), possibly due to the excitation of valence electrons to perturbed states in the aqueous environment. The suppression of resonance involving occupied orbitals may offer information about the availability of certain chemical pathways.

Silver offers an example of one of the several convenient elemental systems that can be studied both as a deposited metal vapour as well as an aqueous ion (AgNO_3 solution), also presenting itself as a relatively high-Z material that can be considered for tracing μXRF systems (Muthuvelu et al., 2004).

Near-edge features (the K-edge for neutral Ag is at 25.517 keV) due to atomic resonance in singly ionised Ag are also evident here (Fig. 3). We note that the elastic scattering minimum and adjacent maximum straddle the energy point associated with the first excitation in

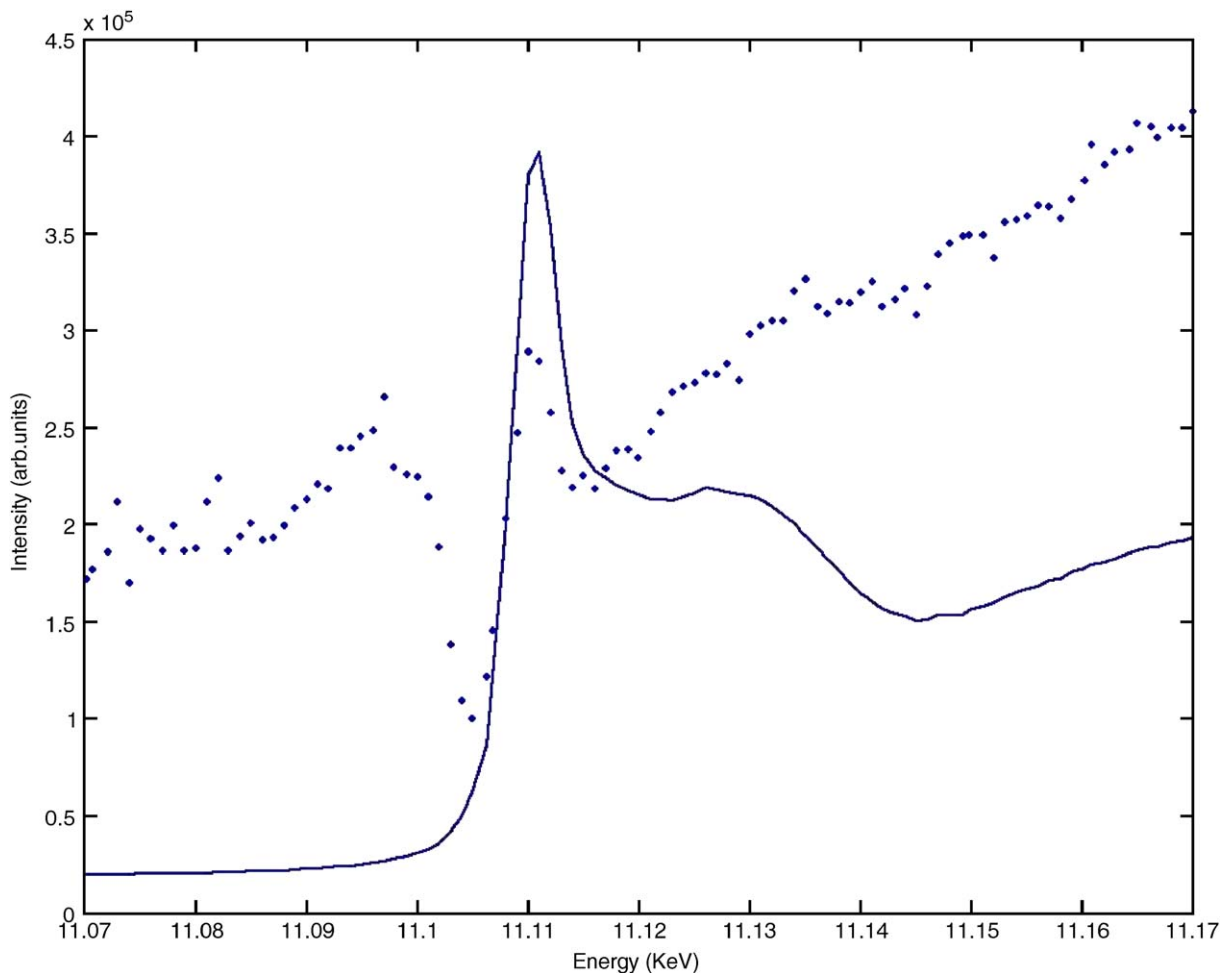


Fig. 3. Results of pilot investigation for an aqueous solution of AgNO_3 , showing near-edge structure in the elastic scattering signal (the lighter line showing the slowly rising absorption edge measured through detection of XRF and the darker line the variation in scattering intensity).

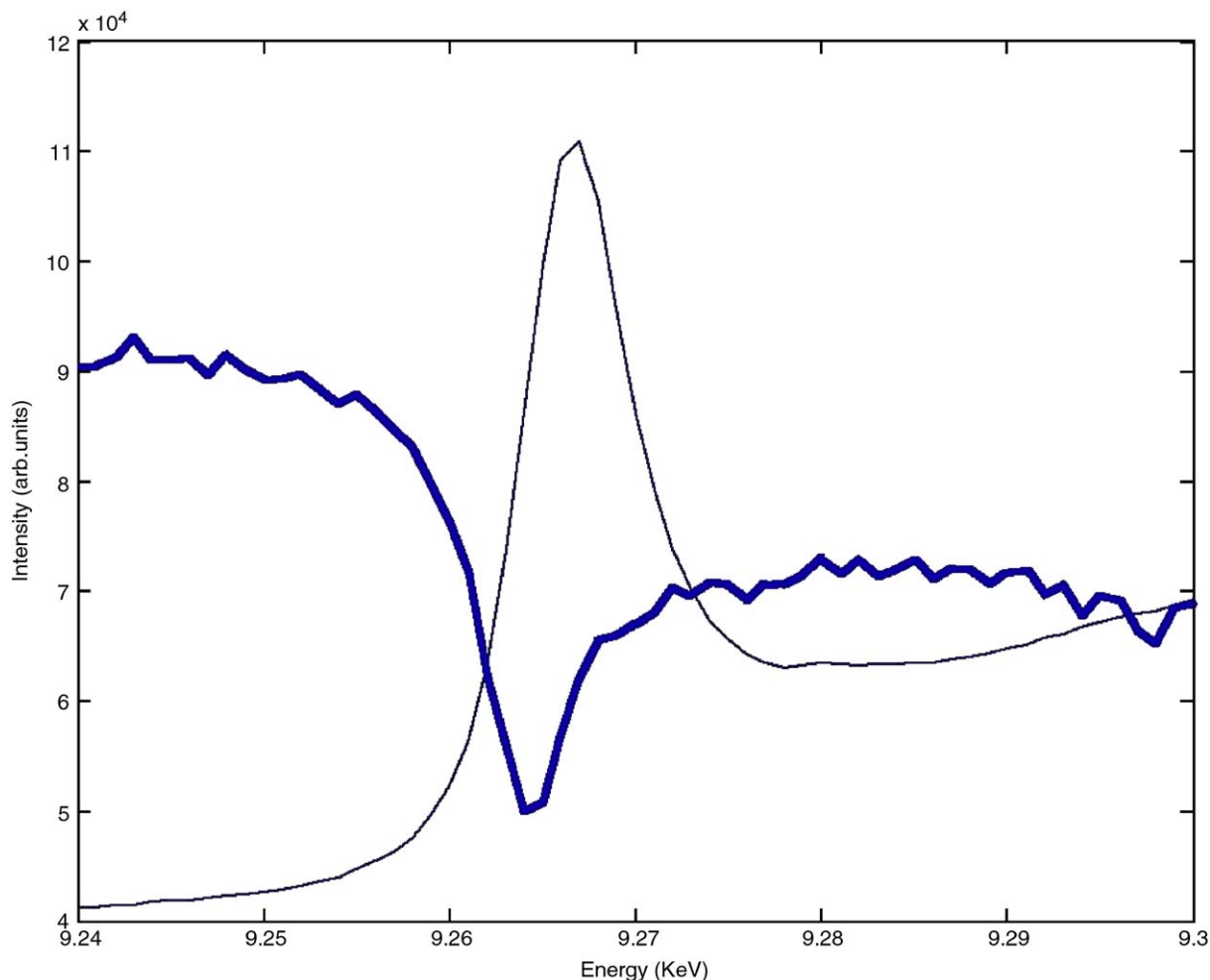


Fig. 4. Elastic scattering (dark line) and fluorescence (light line) in erbium doped sol-gel glass (0.1% by wt).

accord with the dispersion relations. In Fig. 4 we show results for erbium-doped glass, measurements being made in the vicinity of the L-edge (for which the L_{II} absorption edge is at 9.263 keV). Features, in particular the elastic scattering minimum, are evident for the ion embedded in this amorphous system that, like the aqueous system, offers the potential for the preservation of atomic effects. Again the elastic scattering minimum lies at several eV lower energy than fluorescence maximum associated with the first excitation.

5. Conclusions

Third generation synchrotron sources offer tuneable monochromatic X-rays at sufficient intensity to quantitatively evaluate elastic scattering cross-sections at core electron energies for a wide range of elements and

conditions. While data is forthcoming for elastic scattering in gases, there is less data for atoms and ions. Here incomplete valence shells generate complex near-edge scattering structures due to the availability of lower energy bound-bound transitions and the enhancement of oscillator strengths with increasing positive charge. Direct measurement of the ratios of elastic X-ray scattering intensities for constituent atoms, ions and molecules borne in an amorphous system via the method presented in this paper offers good potential for testing IPA theory beyond experiments performed for atoms of noble gases.

Acknowledgement

The authors wish to acknowledge the beneficial advice and encouragement of Prof R. H. Pratt, University of Pittsburgh.

References

- Bijvoet, J.M., 1949. Proc. Kon. Ned. Akad. Wet 52, 313.
- Bijvoet, J.M., Peerdeman, A.F., van Bommel, A.J., 1951. Nature 168, 271–272.
- Bradley, D.A., Roy, S.C., Kissel, L., Pratt, R.H., 1999. Anomalous scattering effects in elastic photon-atom scattering from biomedically important elements. Radiat. Phys. Chem. 56, 175–195.
- Carney, J.P.J., Pratt, R.H., Kissel, L., Roy, S.C., Sen Gupta, S.K., 2000. Rayleigh scattering from excited states of atoms and ions. Phys. Rev. A 61, 052714/14.
- Creagh, D.C., 1984. X-ray interferometer measurements of the anomalous dispersion correction $f'(\omega, 0)$ for some low-Z elements. Phys. Lett. 103A, 52–56.
- Cromer, D.T., Liberman, D., 1970. Relative calculation of anomalous scattering factors for X-rays. J. Chem. Phys. 53, 1891–1989.
- Cullen, D.E., 1989. Program SCATMAN: A Code Designed to Calculate Photon Coherent Scattering Anomalous Scattering Factors and Cross Sections. Lawrence Livermore National Laboratory, UCRL-ID-103422, November.
- Hamalainen, K., Manninen, S., Suortti, P., Collins, S.P., Cooper, M.J., Laundry, D., 1989. Resonant Raman scattering and inner-shell hole widths in Cu, Zn and Ho. J. Phys. Condens. Matter 1, 5955–5964.
- Hugtenburg, R.P., Bradley, D.A., 2004. Anomalous Rayleigh scattering with dilute concentrations of elements of biological importance. Nucl. Instrum Methods Phys. Res. B 213, 552–555.
- Hugtenburg, R.P., Muthuvelu, P., Bradley, D.A., 2002. Anomalous Rayleigh scatter in dilute media. Phys. Med. Biol. 47, 3407–3417.
- Hugtenburg, R.P., Yusoff, A.L., Bradley, D.A., 2004. Near-edge anomalous Rayleigh scattering in Cu ions. Rad. Phys. Chem. 71, 655–666.
- Kissel, L., 2000. RTAB: The Rayleigh scattering database. Radiat. Phys. Chem. 59, 185–200.
- Kissel, L., Zhou, B., Roy, S.C., Sen Gupta, S.K., Pratt, R.H., 1995. The validity of form-factor, modified-form-factor and anomalous-scattering-factor approximations in elastic scattering calculations. Acta Crystallogr A 51, 271–288.
- Liberman, D.A., Cromer, D.T., Waber, J.T., 1971. Relativistic self-consistent field program for atoms and ions. Comput. Phys. Commun. 2, 107–113.
- Muthuvelu, P., Ellis, R.E., Sheldon, B., Attenburrow, D., Barrett, R., Drakopoulos, M., Winlove, C.P., Bradley, D.A., 2004. Investigations of vascularisation and blood flow at the subchondral plate using an X-ray fluorescence technique. Radiat Phys. Chem. 71, 961–962.
- Scofield, J.H., 1969. Radiative decay rates of vacancies in the K and L shells. Phys. Rev. 179, 9–16.
- Scofield, J.H., 1973. Theoretical photoionization cross-sections from 1 to 1500 keV. Lawrence Livermore National Laboratory, UCRL-ID-103422.
- Stohr, J., 1998. NEXAFS Spectroscopy. Springer, Berlin.
- Suortti, P., 1979. Scattering of X-rays near the K absorption edge. I. Fluorescence and resonant Raman scattering in transition metals. Phys. Status Solidi 91, 657–666.
- Templeton, D., 1994. In: Materlik, G., Sparks, C.J., Fischer, K. (Eds.), Resonant Anomalous X-Ray scattering: Theory and applications. Elsevier Science, New York.
- Young, L., Dunford, R.W., Kanter, E.P., Krassig, B., Southworth, S.H., Bonham, R.A., Lykos, P., Morong, C., Timm, A., Carney, J.P.J., Pratt, R.H., 2001. Corrections to the usual X-ray scattering factors in rare gases: experiment and theory. Phys. Rev. A 63, 052718.
- Zhou, B., Kissel, L., Pratt, R.H., 1992. Simple computational schemes for X-ray anomalous scattering factors for ions. Nucl. Instrum. Methods B 66, 307–312.
- Zhou, B., Pratt, R.H., Roy, S.C., Kissel, L., 1990. Calculation of anomalous scattering for ions and atoms. Phys. Scr. 41, 495–498.